

Peripheral Neural Detection of Danger–Associated and Pathogen–Associated Molecular Patterns

Gareth L. Ackland, PhD, FRCA, FFICM¹; Vitaly Kazymov, PhD²; Nephtali Marina, PhD²; Mervyn Singer, MD, FRCP, FFICM¹; Alexander V. Gourine, PhD²

Objective: Bidirectional links between the nervous and immune systems modulate inflammation. The cellular mechanisms underlying the detection of danger-associated molecular patterns and pathogen-associated molecular patterns by the nervous system are not well understood. We hypothesized that the carotid body, a tissue of neural crest origin, detect pathogen associated molecular patterns and danger associated molecular patterns via an inflammasome-dependent mechanism similar to that described in immune cells.

Design: Randomized, controlled laboratory investigation.

Setting: University laboratory.

Subjects: C57Bl/6J mice; juvenile Sprague-Dawley rats, primary human neutrophils.

Interventions: Rat carotid body chemosensitive cells, and human neutrophils, were treated with TLR agonists to activate inflammasome-dependent pathways. In mice, systemic inflammation was induced by the pathogen associated molecular pattern zymosan (intraperitoneal injection; 500 mg/kg). Isolated carotid body/carotid sinus nerve preparations were used to assess peripheral chemoafferent activity. Ventilation was measured by whole-body plethysmography.

Measurements and Main Results: Chemosensitive carotid body glomus cells exhibited toll-like receptor (TLR-2 and TLR-4), NLRP1, and NLRP3 inflammasome immunoreactivities. Zymosan increased NLRP3 inflammasome and interleukin-1 β expression in glomus cells ($p < 0.01$). Human neutrophils demonstrated similar LPS-induced changes in inflammasome expression. Carotid body glomus cells also expressed IL-1 receptor and responded to application of IL-1 β with increases in intracellular [Ca²⁺]. Four hours after injection of zymosan carotid sinus nerve chemoafferent discharge assessed in vitro (i.e., in the absence of acidosis/circulating inflammatory mediators) was increased five-fold ($p < 0.001$). Accordingly, zymosan-induced systemic inflammation was accompanied by enhanced respiratory activity.

Conclusions: In carotid body chemosensitive glomus cells, activation of toll-like receptors increases NLRP3 inflammasome expression, and enhances IL-1 β production, which is capable of acting in an autocrine manner to enhance peripheral chemoreceptor drive. (*Crit Care Med* 2013; 41:e85–e92)

Key Words: autonomic; inflammasomes; inflammation mediators; sepsis; sensory receptor cells

¹Department of Medicine, Bloomsbury Institute of Intensive Care Medicine, Division of Medicine, University College London, London, United Kingdom.

²Department of Neuroscience, Physiology and Pharmacology, University College London, London, United Kingdom.

This work was undertaken at laboratories in University College London.

Supported, in part, by Academy Medical Sciences/Health Foundation Clinician, Scientist Award (Dr. Ackland), UK Intensive Care Society Young Investigator award (Dr. Ackland), and The Wellcome Trust (Dr. Gourine is a Wellcome Trust Senior Research Fellow). Part of this work was undertaken at UCLH/UCL that received a proportion of funding from the UK Department of Health's NIHR Biomedical Research Centre's funding scheme.

Drs. Ackland and Gourine are consultants for Baxter Healthcare.

Drs. Ackland, Kazymov, Marina, Singer, and Gourine received funding from the Academy of Medical Sciences/Health Foundation Clinician Scientist award and the National Institute for Health Research UK.

For information regarding this article, E-mail: g.ackland@ucl.ac.uk and a.gourine@ucl.ac.uk

Copyright © 2013 by the Society of Critical Care Medicine and Lippincott Williams & Wilkins. This is an open access article distributed under the Creative Commons Attribution License, which permits unrestricted use, distribution, and reproduction in any medium, provided the original work is properly cited.

DOI: 10.1097/CCM.0b013e31827c0b05

Inflammasomes have emerged as important cellular complexes involved in the detection of both pathogen-associated molecular patterns (PAMPs) and endogenous danger-associated molecular patterns (DAMPs) by immune cells (1). Once activated, inflammasomes assemble as a cytoplasmic multiprotein complex to activate caspase-1, which proteolytically converts the precursors of proinflammatory cytokines, pro-interleukin (IL)-1 β and pro-IL-18 into active molecules (2). In concert with peripheral immune cell signaling, neural mechanisms orchestrate the inflammatory response via autonomic-immune effector pathways (3). However, the mechanisms underlying detection of PAMPs and DAMPs by the nervous system remain unclear.

The onset of critical illness is frequently accompanied by tachycardia and tachypnea (4). Although these physiological features are commonplace in the critically ill, they often occur in the absence of systemic hypoxia, hypercapnia and/or acidosis (5, 6), major stimuli for increased peripheral

chemoreceptor activity and chemoreceptor-driven cardiovascular and respiratory responses (7), including rapid alterations in heart rate variability (8, 9). Circulating DAMPs, may therefore be an important additional stimulus for increasing peripheral chemoreceptor activity, beyond (and in addition to) previously identified cytokine mediators (10). We therefore hypothesized that chemosensitive glomus cells of the carotid body—a peripheral afferent organ of neural crest origin—are capable of detecting PAMPs/DAMPs by inflammasome activation, to relay immune/inflammatory signals to the central nervous system. We used the yeast cell wall product zymosan, which activates the NLRP3 inflammasome via toll-like receptor-2 (11), to produce a robust model of sterile systemic inflammation in vivo (12, 13) and in cultured cells (12).

MATERIALS AND METHODS

All experiments were performed in accordance with the United Kingdom Animals (Scientific Procedures) Act (1986). All drugs were acquired from Sigma (Poole, UK) unless stated otherwise.

Carotid body Cell Cultures

Sprague-Dawley rat pups (7–11 days old; local breeding colony at University College London) were terminally anesthetized with isoflurane prior to bilateral excision of the carotid bodies (14). Chemosensitive glomus cells were enzymatically isolated by exposing the carotid body tissue to a 0.1% trypsin-0.1% collagenase solution for 1 hr at 37°C followed by mechanical dissociation. The dispersed cell suspension was then collected and triturated in growth medium (F-12 nutrient medium supplemented with 10% (v/v) fetal bovine serum, 80 U/L insulin, 0–6% (w/v) glucose, 2 mM glutamine and 1% penicillin-streptomycin). Dispersed cells were then placed onto poly-L-lysine coated cover slips. Cultures were grown at 37°C in a humidified atmosphere of 95% air/5% CO₂ for 72 hours. Each cell culture contained multiple cell clusters containing approximately 5–30 chemosensitive glomus cells that were easily identified under bright field microscopy. To activate inflammasome-dependent signaling pathways, cultures were incubated in a growth medium containing 0, 0.5, or 5 µg/mL of zymosan for 24 hours.

Primary Human Neutrophils

Primary human neutrophils (>97% purity) were isolated as described previously (12) and incubated with lipopolysaccharide (10 ng/mL; *Escherichia coli* B0111:B4) or phosphate-buffered saline for 1.5 hours prior to cell fixation. Lipopolysaccharide was used since previous studies have shown that in primary human neutrophils the NLRP3 inflammasome is not activated by zymosan (15).

Immunofluorescence Studies

Cell cultures were fixed with 4% paraformaldehyde solution and permeabilized with 0.025% Triton X-100. Blocking solution contained 1% bovine serum albumin and 10% of either

goat or donkey normal serum. Nuclear structures were stained with 4',6-diamidino-2-phenylindole (DAPI). Tyrosine hydroxylase (TH) immunostaining was performed routinely to confirm the glomus cell phenotype. Cultures were simultaneously incubated with sheep anti-TH antibody (1:250 Abcam, Cambridge, UK) with the addition of one of the following antibodies: goat anti-TLR4 (1:500; Santa Cruz, Heidelberg, Germany), rabbit anti-TLR2 (1:250; Santa Cruz), goat anti-IL-1β (epitope mapping at the C-terminus (16, 17); 1:500; Santa Cruz); goat anti-IL-1ra/IL-1F3 (1:250; R & D Systems, Abingdon, UK); rabbit anti-NLRP1 (1:500; Abcam) and goat anti-NLRP3 (1:500, Abcam). Negative controls were performed by the omission of primary or secondary antibodies.

Confocal Microscopy Imaging

Images were captured using a Confocal Laser Scanning Microscope, (Zeiss 510, Welwyn Garden City, UK) with 40X or 60X oil-immersion objectives. UV, argon (458, 477, 488, 504 nm), or helium-neon (543 nm, 633 nm) lasers were used as appropriate. All images were captured using the same settings to enable comparisons of fluorescence intensities between different cell cultures. Intensity of fluorescence was estimated using Zeiss LSM 510 software and expressed in arbitrary units (AU).

Intracellular Ca²⁺ Imaging

Glomus cells were loaded for 40 min at room temperature with Fluo-4 AM (4 µM) or Fura-2 AM (4 µM) to determine changes in cytosolic [Ca²⁺] in response to hypoxia or IL-1β application.

Model of Systemic Inflammation

C57BL/6 inbred mice (~20g; Charles River, UK) received intraperitoneal injections of zymosan (500 mg kg⁻¹; *n* = 12) (12) to induce systemic inflammation or sterile saline (0.2 mL; controls; *n* = 12). Severity scores were recorded as described previously (18).

Whole-body Plethysmography

Ventilation was measured in conscious, freely moving C57BL/6 mice (Charles River, UK) injected with either zymosan or sterile saline (*n* = 5 per group) immediately before being placed in a whole-body plethysmograph, as described previously (13, 18, 19). The recording chamber (250 mL) was flushed continuously with a humidified mixture of 79% nitrogen and 21% oxygen, at a rate of 500 mL/min with temperature maintained at 22°C. Levels of oxygen and carbon dioxide were monitored using a fast-response gas analyzer (Morgan Medical, Hertford, UK). Tidal volume was determined following calibration of the plethysmograph through repeated injections and withdrawal of different volumes of air from within the recording chamber. The mice were left to acclimatize to the chamber environment for at least 30 minutes before measurements of baseline ventilation were taken. Minute ventilation was calculated from the product of *respiratory frequency* and *tidal volume* measurements.

Carotid Sinus Nerve Recordings

Three hours after intraperitoneal injections of zymosan or sterile saline, mice were euthanized under 5% isoflurane anesthesia. The carotid bifurcation region was rapidly removed, placed into a recording chamber (~3 mL), carotid sinus nerve (CSN) was isolated, de-sheathed, and recordings were made using a suction electrode, as described previously (14, 19, 20). Nerve activity signal was amplified ($\times 20,000$) and filtered (200–3,000 Hz), with data acquired and stored using *Spike2* software (Cambridge Electronic Design Ltd, Cambridge, UK). Single-unit analysis was performed offline using the spike-sorting function of *Spike2* software (18). CSN chemoafferent activity was recorded during baseline normoxia and hypoxia, produced by exposure of the preparations to Krebs' solution saturated with 95% N₂/5% CO₂ for 3 minutes. Peak CSN activity was estimated at the end of each experiment by application of sodium cyanide (0.03% w/v; 50 μ L bolus).

Cytokine Measurements

Cytokine levels in plasma were determined using an enzyme-linked immunosorbent assay kit (ProteoPlex Murine CytokineArray, Novagen, Germany), according to manufacturer's instructions. Arterial blood samples were drawn from the carotid artery 3 hours after injection of zymosan. Plasma was separated by centrifugation and stored at -80°C until assayed.

Statistical Analysis

The data were analyzed using GraphPad Prism 5 software. Statistical significance was tested by Student *t* test for paired or unpaired data (two groups) or by repeated measures ANOVA (multiple groups) followed by Tukey-Kramer testing for multiple comparisons between groups. Mean values (\pm SE) are presented, unless stated otherwise. Significance was accepted at *p* values of less than 0.05.

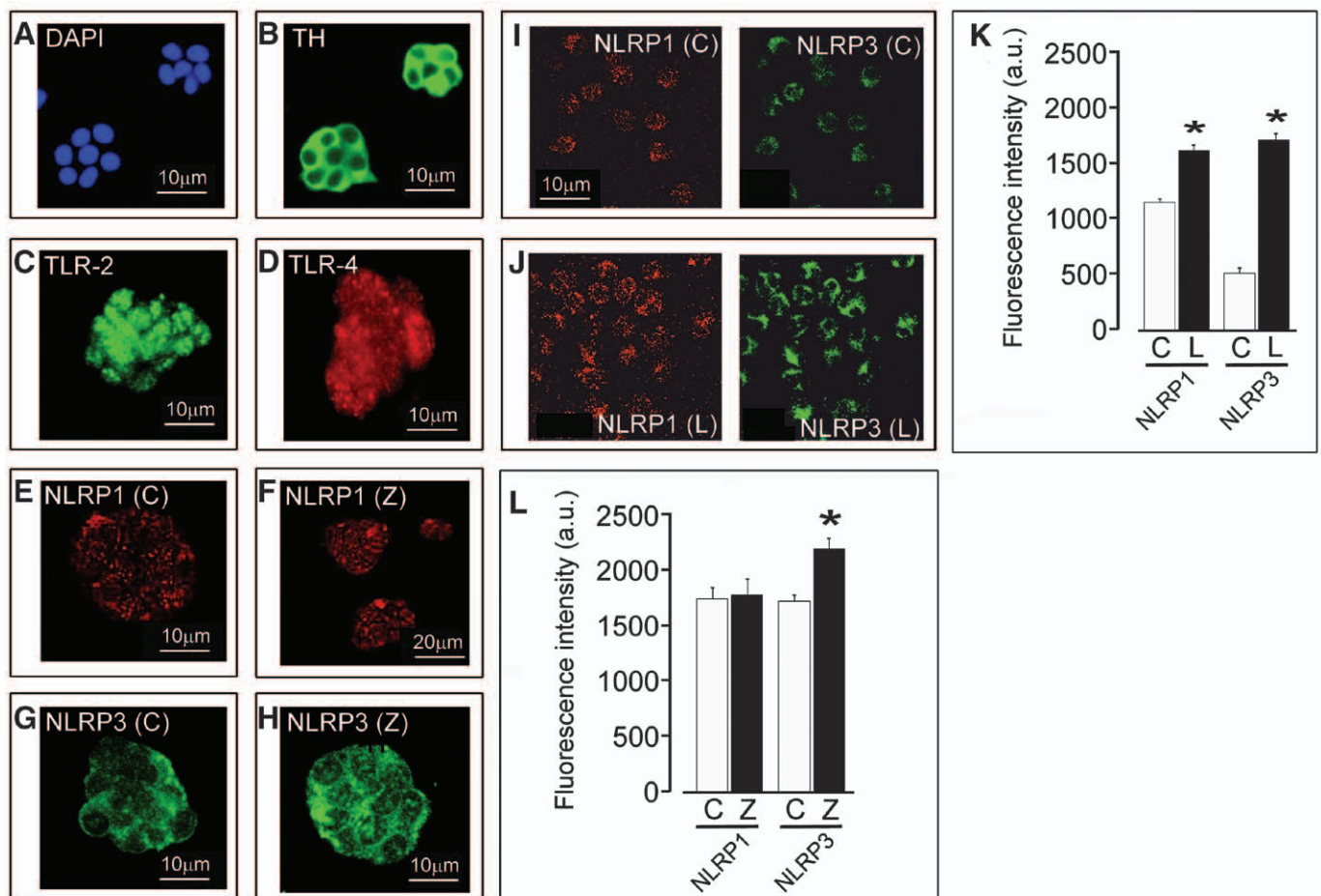


Figure 1. Expression of inflammasome complexes in cultured carotid body glomus cells. **A** and **B**, Representative confocal images showing clusters of the carotid body glomus cells stained with 4',6-diamidino-2-phenylindole and identified on the basis of tyrosine hydroxylase immunoreactivity. **C** and **D**, Toll-like receptor (TLR2 and TLR4) immunoreactivities in glomus cells. **E** and **F**, NLRP1 immunoreactivity in glomus cells following incubation in control medium (C) or in the presence of 500 ng/mL of zymosan (Z). **G** and **H**, NLRP3 immunoreactivity in glomus cells following incubation in control medium (C) or in the presence of 500 ng/mL of zymosan (Z). Note increased immunofluorescence levels in cultures incubated with zymosan. **I** and **J**, NLRP1 and NLRP3 immunoreactivities in primary human neutrophils following incubation in control medium (C) or in the presence of 10 ng/mL of lipopolysaccharide (L). **K**, Summary data showing significant increases in NLRP1 and NLRP3 immunofluorescence intensities in primary human neutrophils in response to lipopolysaccharide (L). **L**, Summary data showing significant increase in NLRP3 immunofluorescence intensity in glomus cells in response to zymosan (Z). Data are presented as means \pm SE. *Significant difference ($p < 0.05$).

RESULTS

Expression of Inflammasome Complexes in Cultured Chemosensitive Carotid Body Glomus Cells

We investigated the presence and changes in the expression level of inflammasomes in cultured chemosensitive glomus cells following incubation with zymosan. Carotid body glomus cells (Fig. 1A and B) were found to display TLR-2 (Fig. 1C), TLR-4 (Fig. 1D), NLRP1 (Fig. 1E) and NLRP3 (Fig. 1G) inflammasome immunoreactivities. NLRP1 staining was found to be dispersed throughout the cell body (Fig. 1E). As reported previously (15), distribution of NLRP3 protein could be different, and in glomus cells being concentrated around the edge of the cell (Fig. 1G). NLRP3 expression by glomus cells was up-regulated (Fig. 1H, I; $p = 0.023$) following incubation with zymosan, whereas expression of NLRP1 was unaffected (Fig. 1F and L). Incubation of primary human neutrophils with lipopolysaccharide induced similar in magnitude increases in the expression of both NLRP1 and NLRP3 inflammasomes (Fig. 1I–K).

Effect of Zymosan on IL-1 β Expression in Chemosensitive Carotid Body Glomus Cells

Incubation of glomus cells in the presence of zymosan (0.5 or 5 $\mu\text{g}/\text{mL}$) resulted in a profound up-regulation of IL-1 β

expression (Fig. 2A and B; $p < 0.0001$). We also confirmed the presence of IL-1 receptor immunoreactivity in glomus cells (Fig. 2C) suggesting that IL-1 β produced by these cells may act in an autocrine manner.

Effect of IL-1 β on $[\text{Ca}^{2+}]_i$ in Chemosensitive Carotid Body Glomus Cells

Next, we confirmed that IL-1 β is capable of eliciting a physiological response in the carotid body glomus cells. As expected, hypoxia activated glomus cells, as characterized by immediate high amplitude increases in $[\text{Ca}^{2+}]_i$ with a rapid return to basal levels shortly after reoxygenation (Fig. 3A and B). In conditions of normoxia, glomus cells were activated in the presence of IL-1 β ($n = 23$ cells; three independent experiments; Fig. 3C and D). Application of IL-1 β induced a delayed $[\text{Ca}^{2+}]_i$ response in glomus cells, which was observed ~ 10 minutes after cytokine application and was characterized by sustained high-amplitude oscillations in $[\text{Ca}^{2+}]_i$. IL-1 β -induced Ca^{2+} responses in glomus cells were abolished in the presence of IL-1 receptor antagonist in the incubation media (Fig. 3E).

Carotid Body Chemoafferent Activity During Systemic Inflammation

Since IL-1 β actions on glomus cells of the carotid body mimicked the effect of hypoxia, we sought in vivo evidence that systemic inflammation augments carotid body chemosensitivity and increases ventilation. Zymosan-treated mice showed classical clinical signs of systemic inflammation, corroborated by high cytokine levels in plasma (Table 1). Arterial blood oxygen (zymosan-treated: 9.1 ± 1.6 kPa; control: 10.0 ± 1.7 kPa) and carbon dioxide tensions (zymosan: PaCO_2 3.5 kPa; control: 3.6 kPa) were similar ($n = 5$ each group). Developing of systemic inflammation following administration of zymosan ($n = 5$) was accompanied by significant increases in respiratory frequency and hence minute ventilation 2 hours after the injections ($p < 0.05$; Fig. 4). Core temperature ($34.9 \pm 1.1^\circ\text{C}$) was lower in mice injected with zymosan (13), compared with mice that received sterile saline ($36.2 \pm 0.9^\circ\text{C}$; $p < 0.05$).

To determine whether zymosan-induced systemic inflammation alters peripheral chemoreceptor activity, we recorded CSN activity in a superfused in vitro carotid body/CSN preparation free of possible confounding factors present in vivo such as metabolic acidosis and circulating inflammatory mediators. Representative examples of chemoafferent activity recorded in the carotid body/CSN preparations taken from the animals injected with saline (control) and zymosan are shown in Fig. 5A. Resting CSN discharge frequency was increased five-fold in preparations taken from zymosan-treated mice ($p = 0.01$; Fig. 5A, B). Chemoafferent responses to hypoxia (Fig. 5A and C) or application of cyanide (Fig. 4D) were also significantly enhanced in the carotid body/CSN preparations of mice injected with zymosan.

CSN chemoafferent activity is composed of individual spikes with distinguishable amplitude and shape (19). This allows analysis and comparison of single-unit chemoafferent activity between control and zymosan-treated mice. Although mean

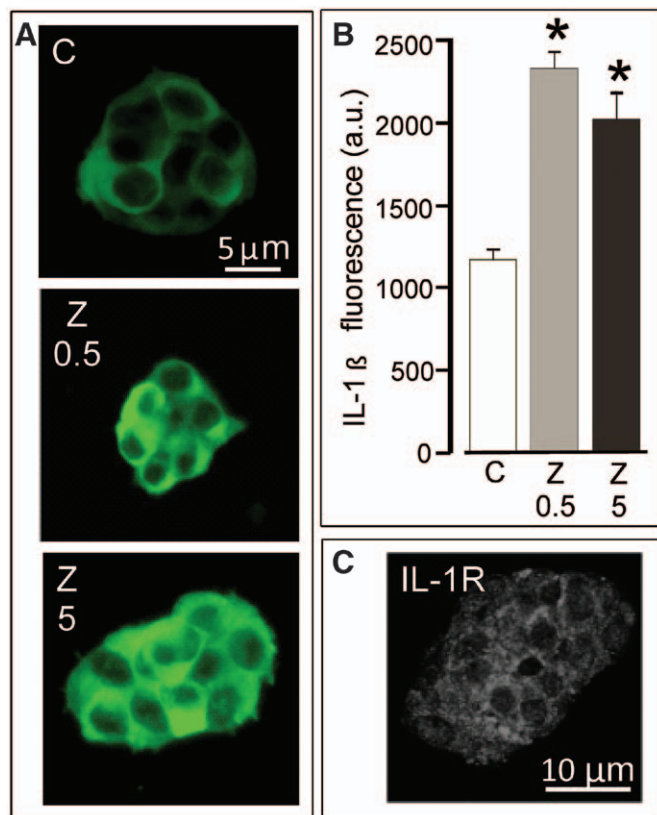


Figure 2. Effects of zymosan on interleukin (IL)-1 β expression in glomus cells of the carotid body. **A**, IL-1 β immunoreactivity in glomus cells following incubation in control medium (C) or in the presence of 0.5 (Z 0.5) and 5 $\mu\text{g}/\text{mL}$ (Z 5) of zymosan. **B**, Summary data showing significant increases in IL-1 β immunofluorescence intensity in glomus cells in response to zymosan. **C**, IL-1 receptor immunoreactivity in glomus cells. Data are presented as means \pm SE. * Significant difference ($p < 0.05$).

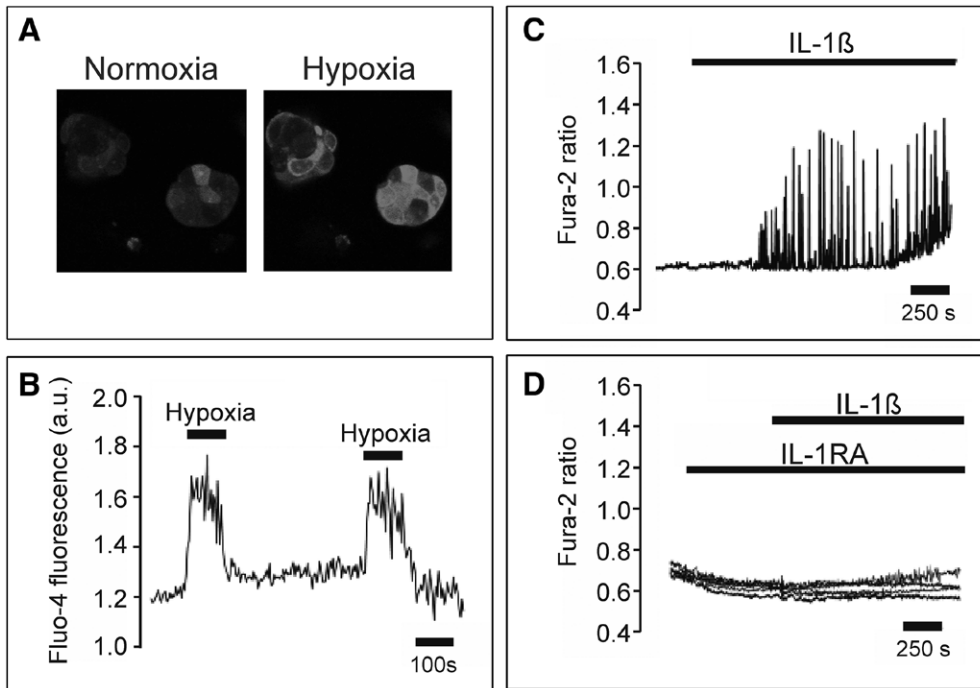


Figure 3. Effects of hypoxia and IL-1 β on [Ca²⁺]_i in glomus cells of the carotid body. **A**, Clusters of glomus cells loaded with the fluorescent Ca²⁺ indicator Fluo-4. Fluorescent images were obtained before (*left panel*) and at the peak of [Ca²⁺]_i response to hypoxia (*right panel*). **B**, Representative trace showing changes in [Ca²⁺]_i elicited in an individual glomus cell in response to hypoxia. **C**, Representative trace showing changes in [Ca²⁺]_i elicited in an individual glomus cell in response to interleukin (IL)-1 β . **D**, IL-1 β -induced [Ca²⁺]_i responses in glomus cells are abolished in the presence of IL-1-receptor antagonist.

discharge frequency of individual CSN fibers increased only in control mice during hypoxia (**Fig. 6A**), the overall higher CSN discharge in mice treated with zymosan was attributable to the recruitment of more individual fibers both at baseline conditions and during hypoxia ($p = 0.0001$; **Fig. 6B**).

DISCUSSION

Chemosensitive glomus cells of the carotid body express both NLRP1 and NLRP3 inflammasomes. When stimulated

TABLE 1. Plasma Cytokine Levels in Mice Injected With Zymosan (500 mg/kg Interperitoneal)

	Saline	Zymosan ($p < 0.001$)
Interleukin-1 β	Below limits of detection	20 \pm 3
Interleukin-6	13 \pm 7	3,800 \pm 991
Interleukin-10	47 \pm 35	382 \pm 46
Tumor necrosis factor- α	112 \pm 12	659 \pm 189
Clinical severity score (range)	0	1–2

All values are mean \pm sd (pg/mL), other than clinical severity score.

with zymosan, glomus cells up-regulate the expression of NLRP3, suggesting that peripheral chemoreceptors of neural crest origin utilize the same mechanism as innate immune cells to detect PAMPs and, potentially, DAMPs. The data obtained also confirm the results of previous studies showing that, in addition to sensing arterial levels of PO₂, PCO₂, and pH, peripheral chemoreceptors are capable of detecting other modalities, including glucose concentration, various electrolytes, neurohormones, and inflammatory mediators (21), many of which are released and/or their levels are altered during systemic inflammation. Indeed, several groups have reported that various proinflammatory cytokines, including TNF α , impact on carotid body chemoreceptor function.

Interestingly, experimental chronic intermittent hypoxia itself increases expression of proinflammatory cytokines within the carotid body, perhaps through oxidative stress (22). The generation of reactive oxygen species is crucial in regulating inflammasome gene expression (23). Here we extend these concepts by demonstrating that inflammasome complexes that detect an array of DAMPs regulate the expression of IL-1 β by the chemosensitive carotid body glomus cells (24).

We have also confirmed recently reported data suggesting that IL-1 β is a cytokine capable of altering carotid body function (25), but have extended this observation by demonstrating one of the possible sources of IL-1 β as the glomus cells themselves following activation of TLR-2 and inflammasome complexes. Critically, the effects of TLR-2 receptor activation by zymosan were observed in an immune cell-free, aseptic carotid body cell culture free of many confounding factors such as hypoxia or inflammatory mediators. In contrast to the reported depressant effects of TNF α on the carotid body chemosensory function (26), IL-1 β (given in pathophysiologically relevant concentrations) was found to trigger [Ca²⁺]_i oscillations in glomus cells, similar in magnitude to the responses elicited by hypoxia. IL-1 β is known to induce expression of the hypoxia-inducible factor(s), which are essential for the maintenance of normal carotid body activity during hypoxia (27). Therefore, IL-1 β appears to mimic the responses of the carotid body to hypoxia and may, therefore, act in an autocrine manner to enhance the peripheral chemoreceptor drive during systemic inflammation.

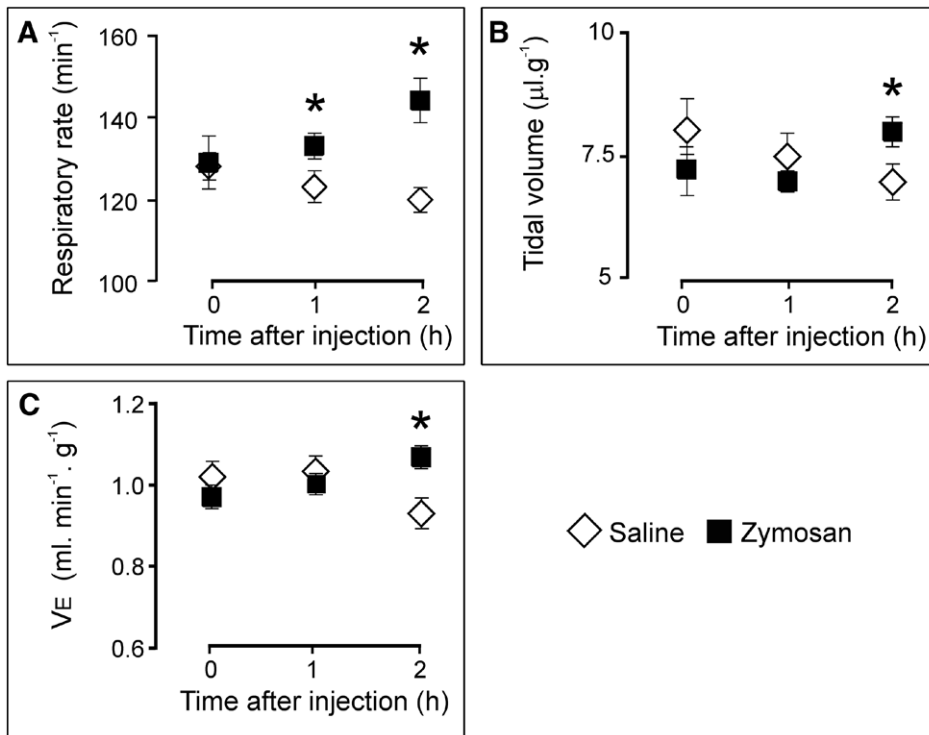


Figure 4. Zymosan-induced systemic inflammation is accompanied by increased ventilatory activity in mice. Group data illustrating changes in the respiratory rate (A), tidal volume (B), and minute ventilation (C) in conscious mice up to 2 hr after intraperitoneal injections of saline or zymosan (500 mg/kg; $n = 5$ per group). Data are presented as means \pm SE. * Significant difference ($p < 0.05$).

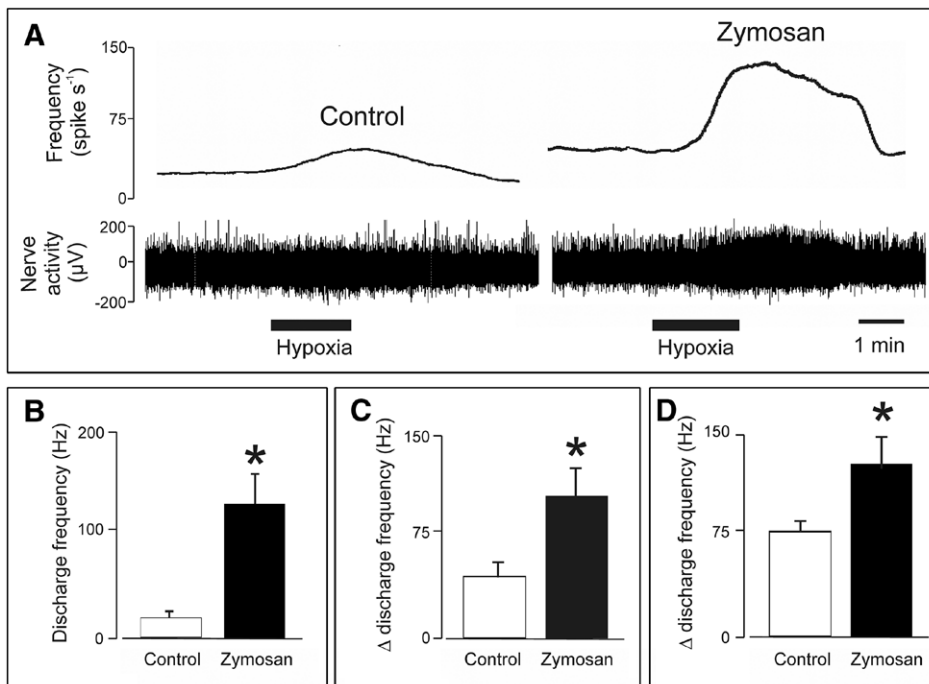


Figure 5. Zymosan-induced systemic inflammation is accompanied by increased carotid body chemoafferent activity. A, Raw data illustrating changes in the carotid sinus nerve chemoafferent activity recorded in the in vitro carotid body/carotid sinus nerve preparations taken 3 hr after intraperitoneal injections of saline (control) or zymosan (500 mg/kg). B–D, Population data [$n = 7$ mice per group] demonstrating that the development of systemic inflammation in response to zymosan leads to higher baseline (A), hypoxia (B) and cyanide induced (C) chemoafferent discharge. C and D, Data are shown as absolute increases from the baseline level of activity. Data are presented as means \pm SE. *Significant difference ($p < 0.05$).

What are the possible implications of inflammatory mediator-dependent alterations in the peripheral chemosensory function on autonomic and neurohormonal control? In this study we show that peripheral chemoafferent activity in normoxia and in conditions of hypoxia is markedly enhanced during early systemic exposure to inflammatory stimuli. Consistent with these data, chronic (proinflammatory) bleomycin-induced lung injury is accompanied by higher baseline respiratory rate and augmented hypoxic ventilatory response (28). The marked increase in the carotid body chemoafferent activity during early systemic inflammation implies that peripheral chemoreceptors may play a key role in the pathophysiology of early sepsis, perhaps by affecting several homeokinetic mechanisms that underlie biological variability. Carotid sinus denervation is associated with shorter survival time in rats administered lethal doses of endotoxin (29), although the impact of concomitant baro-denervation and consequent disruption of baroreflex mechanisms considerably complicate interpretation of any possible protective role of peripheral chemoreceptors.

Clinical data have revealed an association between peripheral chemoreflex dysfunction and outcome from critical illness (30, 31). It is striking, however, that an array of the commonest respiratory, cardiovascular, endocrine, and renal responses observed in critically ill patients can also be produced by discrete activation of the carotid chemoreflex (7). In addition to tachypnea and an increased depth of breathing, peripheral chemoreceptor stimulation results in increased airway resistance and secretions (32). Release of neurohormones, including cortisol and vasopressin, is also increased in response to hypoxemia and carotid sinus activation (5). Clinically, such alterations in autonomic

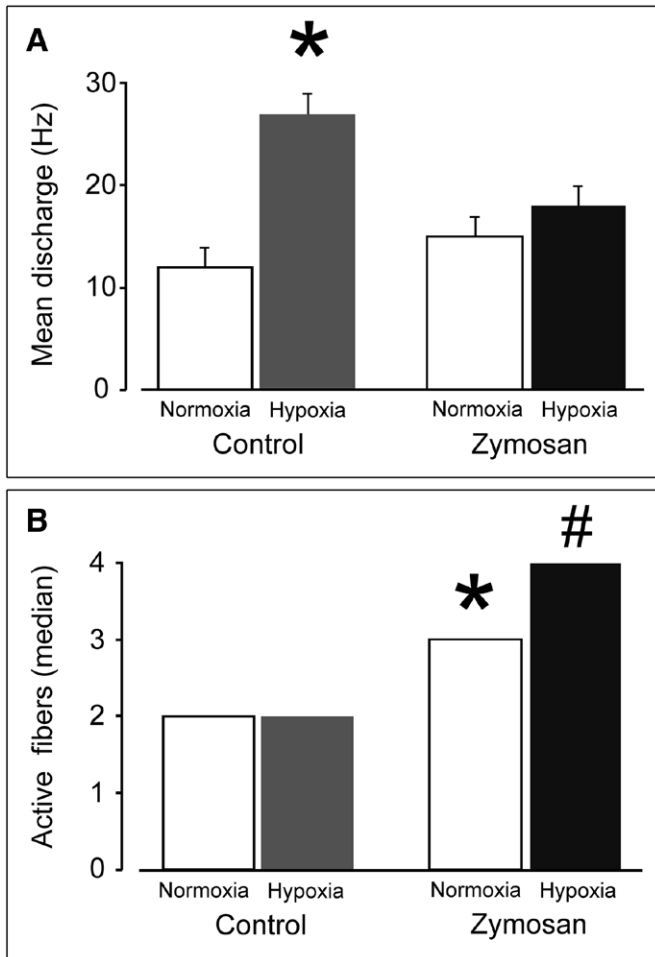


Figure 6. Single-unit analysis of carotid sinus nerve discharge. **A**, Discharge frequency of individual fibers only increases in controls. Data are presented as mean \pm SE. * Significant difference ($p < 0.01$; [$n = 7$ mice per group]). **B**, More single units are recruited in preparations taken from zymosan-treated mice during normoxic (* $p = 0.0001$) and hypoxic (# $p = 0.0001$) conditions ($n = 7$ mice per group).

neural control are detected by profound changes in heart rate variability (4, 8).

CONCLUSION

Perturbations of autonomic control mechanisms are likely to play a key role at the onset of critical illness (8). The early detection of blood-borne DAMPs and PAMPs by the carotid chemoreceptors and the consequent inflammasome-dependent cytokine-induced activation of the peripheral chemoreflex are likely to play a pivotal role in triggering autonomic dysregulation. Understanding how afferent function is altered during systemic inflammation and sepsis may provide novel therapeutic opportunities and/or monitoring modalities (33) to explore.

REFERENCES

- Cinell I, Opal SM: Molecular biology of inflammation and sepsis: A primer. *Crit Care Med* 2009; 37:291–304
- Guarda G, So A: Regulation of inflammasome activity. *Immunology* 2010; 130:329–336
- Tracey KJ: Physiology and immunology of the cholinergic antiinflammatory pathway. *J Clin Invest* 2007; 117:289–296
- Korach M, Sharshar T, Jarrin I, et al: Cardiac variability in critically ill adults: influence of sepsis. *Crit Care Med* 2001; 29:1380–1385
- Rangel-Frausto MS, Pittet D, Costigan M, et al: The natural history of the systemic inflammatory response syndrome (SIRS). A prospective study. *JAMA* 1995; 273:117–123
- Godin PJ, Fleisher LA, Eidsath A, et al: Experimental human endotoxemia increases cardiac regularity: Results from a prospective, randomized, crossover trial. *Crit Care Med* 1996; 24:1117–1124
- Marshall JM: Peripheral chemoreceptors and cardiovascular regulation. *Physiol Rev* 1994; 74:543–594
- Godin PJ, Buchman TG: Uncoupling of biological oscillators: A complementary hypothesis concerning the pathogenesis of multiple organ dysfunction syndrome. *Crit Care Med* 1996; 24:1107–1116
- Annane D, Trabold F, Sharshar T, et al: Inappropriate sympathetic activation at onset of septic shock: A spectral analysis approach. *Am J Respir Crit Care Med* 1999; 160:458–465
- Zapata P, Larrain C, Reyes P, et al: Immunosenory signalling by carotid body chemoreceptors. *Respir Physiol Neurobiol* 2011; 178:370–374
- Lamkanfi M, Malireddi RK, Kanneganti TD: Fungal zymosan and mannan activate the cryopyrin inflammasome. *J Biol Chem* 2009; 284:20574–20581
- Ackland GL, Gutierrez Del Arroyo A, Yao ST, et al: Low-molecular-weight polyethylene glycol improves survival in experimental sepsis. *Crit Care Med* 2010; 38:629–636
- Volman TJ, Goris RJ, van der Jagt M, et al: Organ damage in zymosan-induced multiple organ dysfunction syndrome in mice is not mediated by inducible nitric oxide synthase. *Crit Care Med* 2002; 30:1553–1559
- Trapp S, Aller MI, Wisden W, et al: A role for TASK-1 (KCNK3) channels in the chemosensory control of breathing. *J Neurosci* 2008; 28:8844–8850
- Kummer JA, Broekhuizen R, Everett H, et al: Inflammasome components NALP 1 and 3 show distinct but separate expression profiles in human tissues suggesting a site-specific role in the inflammatory response. *J Histochem Cytochem* 2007; 55:443–452
- Descamps D, Le Gars M, Balloy V, et al: Toll-like receptor 5 (TLR5), IL-1 β secretion, and asparagine endopeptidase are critical factors for alveolar macrophage phagocytosis and bacterial killing. *Proc Natl Acad Sci USA* 2012; 109:1619–1624
- Mizutani N, Nabe T, Yoshino S: Complement C3a regulates late asthmatic response and airway hyperresponsiveness in mice. *J Immunol* 2009; 183:4039–4046
- Brealey D, Karyampudi S, Jacques TS, et al: Mitochondrial dysfunction in a long-term rodent model of sepsis and organ failure. *Am J Physiol Regul Integr Comp Physiol* 2004; 286:R491–R497
- Trapp S, Tucker SJ, Gourine AV: Respiratory responses to hypercapnia and hypoxia in mice with genetic ablation of Kir5.1 (Kcnj16). *Exp Physiol* 2011; 96:451–459
- Rong W, Gourine AV, Cockayne DA, et al: Pivotal role of nucleotide P2X2 receptor subunit of the ATP-gated ion channel mediating ventilatory responses to hypoxia. *J Neurosci* 2003; 23:11315–11321
- Kumar P, Bin-Jalil I: Adequate stimuli of the carotid body: More than an oxygen sensor? *Respir Physiol Neurobiol* 2007; 157:12–21
- Del Rio R, Moya EA, Parga MJ, et al: Carotid body inflammation and cardiorespiratory alterations in intermittent hypoxia. *Eur Respir J* 2012; 39:1492–1500
- Gross O, Thomas CJ, Guarda G, et al: The inflammasome: An integrated view. *Immunol Rev* 2011; 243:136–151
- Sutterwala FS, Ogura Y, Flavell RA: The inflammasome in pathogen recognition and inflammation. *J Leukoc Biol* 2007; 82:259–264
- Shu HF, Wang BR, Wang SR, et al: IL-1 β inhibits IK and increases [Ca²⁺]_i in the carotid body glomus cells and increases carotid sinus nerve firings in the rat. *Eur J Neurosci* 2007; 25:3638–3647

26. Fernández R, González S, Rey S, et al: Lipopolysaccharide-induced carotid body inflammation in cats: Functional manifestations, histopathology and involvement of tumour necrosis factor-alpha. *Exp Physiol* 2008; 93:892–907
27. Hellwig-Bürgel T, Rutkowski K, Metzen E, et al: Interleukin-1beta and tumor necrosis factor-alpha stimulate DNA binding of hypoxia-inducible factor-1. *Blood* 1999; 94:1561–1567
28. Jacono FJ, Peng YJ, Nethery D, et al: Acute lung injury augments hypoxic ventilatory response in the absence of systemic hypoxemia. *J Appl Physiol* 2006; 101:1795–1802
29. Tang GJ, Kou YR, Lin YS: Peripheral neural modulation of endotoxin-induced hyperventilation. *Crit Care Med* 1998; 26:1558–1563
30. Schmidt H, Müller-Werdan U, Hoffmann T, et al: Autonomic dysfunction predicts mortality in patients with multiple organ dysfunction syndrome of different age groups. *Crit Care Med* 2005; 33:1994–2002
31. Schmidt H, Hoyer D, Hennen R, et al: Autonomic dysfunction predicts both 1- and 2-month mortality in middle-aged patients with multiple organ dysfunction syndrome. *Crit Care Med* 2008; 36: 967–970
32. Taylor EW, Jordan D, Coote JH: Central control of the cardiovascular and respiratory systems and their interactions in vertebrates. *Physiol Rev* 1999; 79:855–916
33. Cooke WH, Rickards CA, Ryan KL, et al: Autonomic compensation to simulated hemorrhage monitored with heart period variability. *Crit Care Med* 2008; 36:1892–1899